Research Article

Jiahui Li, Yangfeng Wang, Xuehua He, Qing Sun, Meichai Xiong, Zichong Chen, Chengfu Zeng, Xiaohua Zheng, and Chu Liang*

A facile and universal method to purify silica from natural sand

https://doi.org/10.1515/gps-2022-0079 received May 16, 2022; accepted August 22, 2022

Abstract: The major constituents of sand are silica and silicates. The facile and low-cost purification technology of silica from natural sand is of magnificent importance to the industrial applications of silicon-based materials. Herein, we report a green, low-cost, and universal method to purify silica from natural sand. Sand from deserts, rivers, and seas is selected as the representative of natural sand. The initial purity of silica is 52.1 wt% for desert sand, 39.3 wt% for river sand, and 35.8 wt% for sea sand. Highpurity silica has been successfully separated and purified from natural sand via ball milling, reacting with 30 bar CO₂ and hydrochloric acid. The purity of silica derived from natural sand reaches >96 wt%. In this work, the mechanism for the purification of silica from natural sand is discussed. This study provides a new method to separate high-purity silica from natural sand without the generation of toxic and harmful substances.

Keywords: silica, natural sand, purification, metal silicate, CO₂

Jiahui Li, Yangfeng Wang, Xuehua He, Qing Sun, Meichai Xiong, Chengfu Zeng, Xiaohua Zheng: College of Materials Science and Engineering, Zhejiang University of Technology, Hangzhou, 310014, China

Zichong Chen: College of Materials Science and Engineering, Zhejiang University of Technology, Hangzhou, 310014, China; State Key Lab of Silicon Materials, Zhejiang University, Hangzhou, 310027, China

1 Introduction

Silica has been widely used in both industrial products and personal consumption because of its stability and excellent physical and chemical properties. Most of the silica is commercially used as the structural material in the architecture industry [1]. Silica is also used as a raw material to prepare glass, silicon, ceramics, optical fibers, and a common additive in food and cosmetics production [2–6]. In addition, silica has broad application prospects in environmental remediation [7], energy conversion and storage [8-10], high-performance catalysts [11-14], pharmaceutical [15-17], and biological technology [18-20] due to its morphology and microstructure diversity. Silica has played an increasingly important role in advanced materials fields due to its low cost, good environmental compatibility, and unique physical and chemical properties. With the progress of advanced preparation technology and the extension of application fields, the market demand for silica, especially for high-purity silica, will rapidly increase in the near future.

Typically, silica can be separated from natural resources or prepared from silicon precursors. Direct mining of highpurity quartz ore is the simplest method to obtain highpurity silica. But the high-purity quartz ore is a rare natural resource in the world. Therefore, recycling and reusing waste and natural materials is a feasible strategy [21-23]. Quartz minerals with impurities such as quartz ore and seabed sedimentary sand can also be used to produce high-purity silica. Acid-base leaching and high-temperature molten salt calcination are the required processes to remove impurities from quartz ore in industry. High-purity silica is finally prepared by the precipitation method through enriched silicate. However, this method is energy-consuming, of high cost, and has poor environmental compatibility. Alternatively, high-purity silica can be obtained synthetically. Many chemical routes have been explored to prepare high-purity silica from various organic and inorganic compounds containing the silicon element, including tetraethyl orthosilicate, hexamethyldisiloxane, Na₂Si₃O₇, Si,

^{*} Corresponding author: Chu Liang, Zhejiang Carbon Neutral Innovation Institute & College of Materials Science and Engineering, Zhejiang University of Technology, Hangzhou, 310014, China; State Key Lab of Silicon Materials, Zhejiang University, Hangzhou, 310027, China, e-mail: cliang@zjut.edu.cn

SiH₄, SiCl₄, etc. [24–32]. Silica was successfully prepared from tetraethyl orthosilicate via three methods: heating at 680–730°C [28], chemical vapor deposition [33], and hydrolysis reactions [29,34]. Among them, the hydrolysis reaction is the most commonly used method for synthesizing silica with various morphologies. The hydrolysis reaction can be described by the following equation [29]:

$$Si(OC_2H_5)_4 + 2H_2O \rightarrow SiO_2 + 4CH_3CH_2OH$$
 (1)

in which the morphology of silica is strongly dependent on the synthesis conditions. The synthesis of silica derived from tetraethyl orthosilicate and hexamethyldisiloxane is of high cost and environmentally incompatible. Moreover, conversion of Si, SiH₄, or SiCl₄ into silica is a chemical route with little practical value owing to their high cost.

It is well known that silica is the major constituent of natural sand. Therefore, natural sand is considered the most abundant and low-cost natural resource for obtaining silica. In this work, we develop a green, low-cost, and universal method to purify silica from natural sand with silica content lower than 55 wt%. The purification procedures include ball milling, reacting with $\rm CO_2$ and hydrochloric acid, and washing with deionized water. High-purity silica with a purity of >96 wt% is successfully separated from desert sand, river sand, and sea sand from different regions. The purification mechanism of silica from natural sand is revealed in this work as well.

2 Materials and methods

 ${
m CO_2}$ (99.995%, Jingong) and hydrochloric acid (HCl, AR, Sinopharm) were used as-received. The sand used in this work was obtained from nature, namely desert sand (KuBuJi Desert, China), river sand (Tingpang River, China), and sea sand (Jiantiao Seaport, China). Before use, the sand was

washed with deionized water and then dried at 80°C for 24 h under vacuum to remove soluble impurities.

To reduce particle size and remove the impurities of the raw sand, it was milled at 500 rpm for 36 h. After ball milling, the sand was then subjected to a purification process. Three methods were employed to purify the post-milled sand. In the first method, HCl hydrothermal treatment was used to remove impurities. The post-milled sand and 3 M HCl were added to the Teflon-lined autoclave for 24 h at 180°C. After the hydrothermal treatment, the obtained solid product was washed with deionized water several times to obtain pure silica. In the second method, CO₂ hydrothermal treatment and HCl washing were used to remove impurities. The sand and deionized water were added to the Teflon-lined autoclave filled with 30 bar CO₂ for 24 h at 180°C with a mass ratio of 1:2. After hydrothermal treatment, the obtained solid product was further soaked in 3 M HCl for 6 h at 25°C, and then washed with deionized water several times to obtain pure silica. In the third method, CO₂ and HCl hydrothermal treatment were used to remove impurities. The sand and deionized water were added to the Teflon-lined autoclave filled with 30 bar CO₂ for 24 h at 180°C with a mass ratio of 1:2. Subsequently, the solid product was further hydrothermally treated with 3 M HCl for 24 h at 180°C. After hydrothermal treatment, the obtained solid product was washed with deionized water several times to obtain pure silica. In order to demonstrate a facile and universal method to purify silica from three natural sand samples, the purification condition parameters, including CO2 pressure, reaction temperature, and reaction time applied in this work, are set higher or longer than the best conditions. Meanwhile, the best purification conditions are also different for desert sand, river sand, and sea sand because of their different compositions and phases.

The XRD patterns of sand were measured using a PANalytical X'Pert PRO X-ray diffractometer with Cu K α radiation (λ = 0.15418 nm). The microstructure

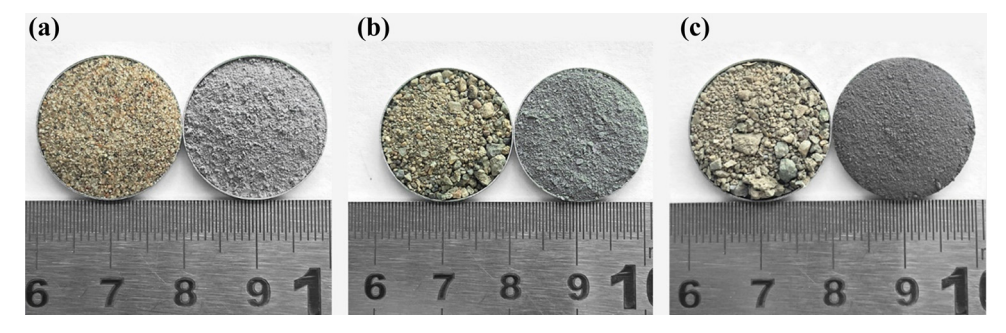


Figure 1: Pictures of the raw sand and post-milled sand samples: (a) desert sand, (b) river sand, and (c) sea sand. The left side is the raw sand and the right side is the post-milled sand.

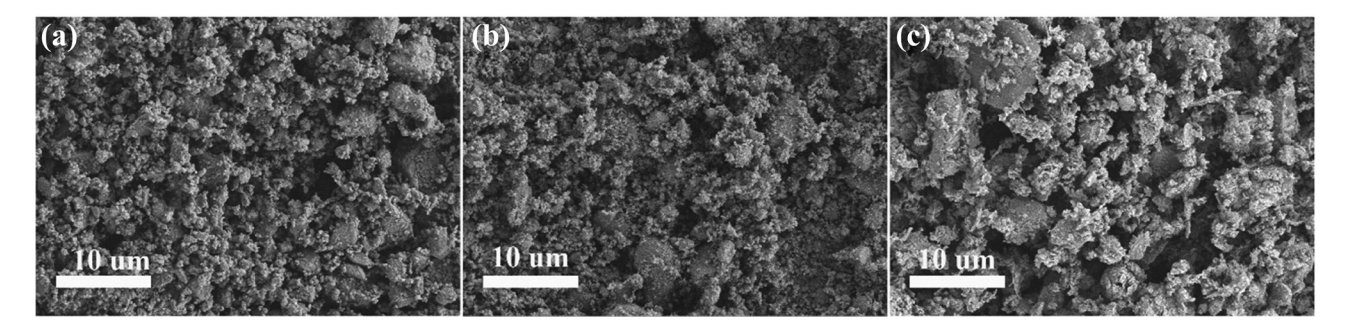


Figure 2: SEM images of post-milled sand samples: (a) desert sand, (b) river sand, and (c) sea sand.

and elemental content of sand and other samples were characterized by scanning electron microscopy (SEM, HITACHI Regulus 8100) with energy-dispersive X-ray spectroscopy (EDS, Oxford X-Max 80 SSD).

3 Results and discussion

Figure 1 shows the pictures of raw materials of desert sand, river sand, and sea sand. It can be clearly observed that the particle sizes of all three kinds of natural sand are very large, and their distribution is uneven, which is not conducive to the following purification. Before purification experiments, therefore, all raw sand is pretreated by high-energy ball milling. After ball milling, the average particle sizes of all the three kinds of sand are found to decrease from several millimeters for the raw sand samples (Figure 1) to submicron for the post-milled sand samples, and their distribution is relatively more even (Figure 2). As shown in Figure 3, the major XRD

peaks centered at 20.8° and 26.6° are seen in the XRD patterns of the post-milled sand samples, which can be attributed to the characteristic peaks of SiO₂ (PDF#85-0798), implying that all the sand samples consist mainly of silica. Moreover, many weak diffraction peaks can be seen in the 2θ range of 20–35°, most of which can be attributed to metal silicates (such as Mg₂(Si₂O₆), Ca₂Mg(Si₂O₇), and Ca(Al₂Si₂O₈)). It should be noted that the XRD peaks of metal carbonates are not observed in the XRD patterns of three sand samples, which may have resulted from their low degree of crystallization in the sand samples. In this work, the first step is to convert silicate anions of metal silicates into silica via designing chemical reactions; the second step is to obtain high-purity silica by removing the impurities in sand samples.

Three post-milled sand samples were collected for composition analysis. The EDS results of desert sand, river sand, and sea sand are listed in Table 1. Obviously, C, O, Mg, Al, Si, K, Ca, and Fe elements are detected in the aforementioned three sand samples. However, the proportion of each element is different for desert sand, river

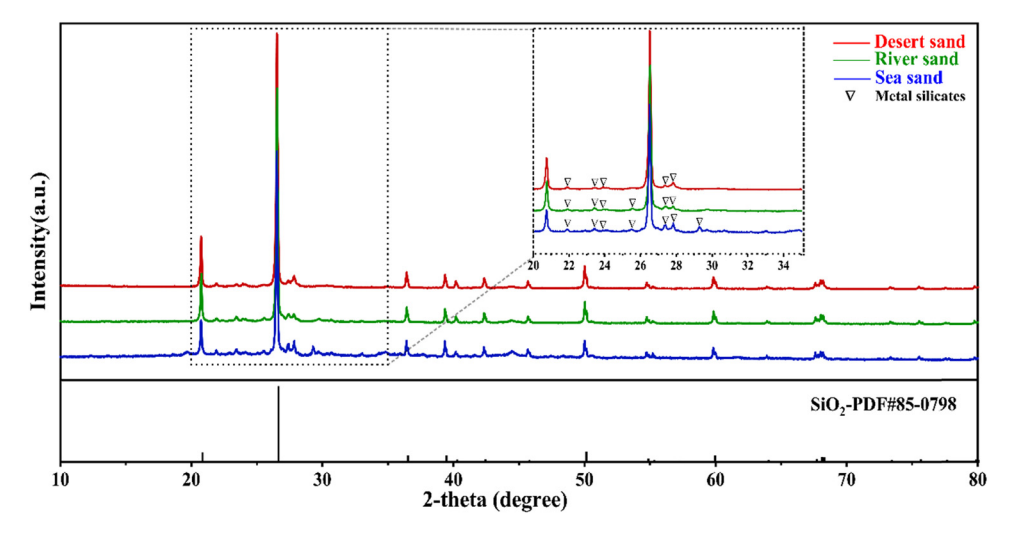


Figure 3: X-ray diffraction analysis of the three kinds of sand after 8 h of high-energy mechanical ball milling.

Table 1: EDS results of the three post-milled sand samples

| Element | Desert sand | | River sand | | Sea sand | |
|---------|-------------|------|------------|------|----------|------|
| | wt% | at% | wt% | at% | wt% | at% |
| С | 26.4 | 36.7 | 34.6 | 46.2 | 12.8 | 20.2 |
| 0 | 44.8 | 46.7 | 40.2 | 40.3 | 44.7 | 53.1 |
| Mg | 0.5 | 0.3 | 0.2 | 0.1 | 0.6 | 0.5 |
| Al | 1.5 | 0.9 | 2.3 | 1.4 | 14.6 | 10.3 |
| Si | 24.3 | 14.4 | 18.3 | 10.4 | 16.7 | 11.3 |
| K | 0.6 | 0.3 | 1.5 | 0.6 | 6.3 | 3.1 |
| Ca | 0.7 | 0.3 | 1.0 | 0.5 | 1.0 | 0.5 |
| Fe | 1.2 | 0.4 | 1.9 | 0.5 | 3.3 | 1.0 |

sand, and sea sand, which is also one of the reasons for the different peak intensities of impurity in XRD patterns. From the combined EDS results with XRD results (Figure 3), it can be seen that Si and C elements are bonded with the other elements in the form of silica, metal silicates, and metal carbonates. Silica is still the main component of the desert sand, the river sand, and the sea sand, which is in good agreement with the XRD results. The atom ratio of oxygen to silicon is 3.2 for desert sand, 3.9 for river sand, and 4.7 for sea sand, respectively, indicating the presence of metal silicates and metal carbonates in the sand samples. According to the content of silicon element in the sand and the chemical formula of silica (SiO₂), the mass fraction of silica is calculated to be 52.1 wt% for desert sand, 39.3 wt% for river sand, and 35.8 wt% for sea sand. The post-milled sand samples are regarded as pristine samples to further design and perform purification experiments.

For the post-milled sand samples, the desert sand and the sea sand have the highest and lowest content of silica, respectively. Table 1 shows that C, Mg, Al, K, Ca, and Fe are the main impurity elements for the three sand samples. The river sand has the highest carbon content of 34.6 wt% and the sea sand has the lowest carbon content of 12.8 wt%, supporting the presence of metal carbonates in the sand samples. Hydrochloric acid was firstly designed to remove the impurity in the sand samples. After reacting sand samples with hydrochloric acid

at 180°C (Experiment 1), the content of silica in all sand samples remarkably increases because of the reduction of impurity elements (Table 2). The silica content of the river sand reaches 97.1 wt%, which is the highest purity among the three sand samples. In contrast, the mass fraction of silica only increases from 52.1 wt for the post-milled desert sand to 78.2% for the desert sand reacted with hydrochloric acid, which is the lowest increase among the three sand samples. The largest increase in silica content is 57.8 wt% for the river sand sample in which this increase in silica content is very close to 54.2 wt% for the postmilled sea sand sample. Moreover, the atom ratio of oxygen to silicon is found to be significantly decreased for the three sand samples after hydrochloric acid treatment (Table 3). The value is 2.8 for the desert sand, 2.0 for the river sand, and 2.2 for the sea sand, implying that most of the metal silicates and metal carbonates are removed from the river sand and sea sand. As a result, it can be concluded that most impurities in the river sand and sea sand samples are removed by reacting with hydrochloric acid. It should be noted that a small amount of impurity is needed further to separate from the sand sample by developing a new purification technology for sand. Even though the river sand has the highest silica content of 97.1 wt% among the three sand samples, it still contains 3.3 wt% metal impurities. Compared with the carbon content and atom ratio of oxygen to silicon (Table 1), it can be known that the metal silicates and metal carbonates in desert

Table 2: Mass fraction of silica in three kinds of post-milled sand treated by different methods

| | | Desert sand (wt%) | River sand (wt%) | Sea sand (wt%) |
|--------------|------------------------------------|-------------------|------------------|----------------|
| Post-milled | | 52.1 | 39.3 | 35.8 |
| Experiment 1 | (HCl@180°C) | 78.2 | 97.1 | 90.0 |
| Experiment 2 | (CO ₂ @180°C) | 44.7 | 37.7 | 29.3 |
| | (CO ₂ @180°C-HCl@25°C) | 87.6 | 76.6 | 79.8 |
| Experiment 3 | (CO ₂ @180°C-HCl@180°C) | 98.4 | 98.3 | 96.8 |

| Element | Desert sand | | River sand | | Sea sand | |
|---------|-------------|------|------------|------|----------|------|
| | wt% | at% | wt% | at% | wt% | at% |
| 0 | 58.3 | 71.1 | 51.4 | 65.0 | 52.2 | 65.9 |
| Mg | 0.3 | 0.3 | 0.0 | 0.0 | 0.0 | 0.0 |
| Al | 3.8 | 2.8 | 2.8 | 2.1 | 3.7 | 2.7 |
| Si | 36.5 | 25.4 | 45.3 | 32.7 | 42.0 | 30.3 |
| K | 1.0 | 0.4 | 0.5 | 0.2 | 2.2 | 11 |

Table 3: Energy-dispersive spectrometer analysis of the three kinds of sand in Experiment 1

sand are more than those in river sand and sea sand. For the desert sand sample, the metal silicates on the particle surface are easy to react with hydrochloric acid to convert into metal chloride and silica. In contrast, the metal silicates in the inner particles are difficult to react with hydrochloric acid because of the sluggish kinetics. Therefore, the silica content of the desert sand in Experiment 1 is much lower than that of the other two sands.

In order to increase the reaction rate of the impurity in sand with the acid, the hydrochloric acid was replaced by 30 bar $\rm CO_2$ and water in Experiment 2 ($\rm CO_2@180^{\circ}C$) because the conversion of metal silicates into silica can be accelerated by introducing high-pressure $\rm CO_2$. The EDS results are listed in Table 2. After reacting pristine sand samples with 30 bar $\rm CO_2$ and water at 180°C in Experiment 2 ($\rm CO_2@180^{\circ}C$), the mass fraction of silica in the sand samples is 44.7 wt% for the desert sand,

37.7 wt% for the river sand, and 29.3 wt% for the sea sand. For the desert sand sample, the purity of silica of 44.7 wt% from the reaction with 30 bar CO₂ and water is much lower than that (78.2 wt%) from the reaction with hydrochloric acid, and that (52.1 wt%) for the post-milled sample. The purity of silica in river sand and sea sand samples is much lower than that of the sand samples reacted with hydrochloric acid but is close to that of the pristine sand samples. These phenomena resulted from the chemical reaction of metal silicates with CO₂. In order to confirm the conversion reaction of metal silicates into silica by reacting with CO2, a CaSiO3-CaCO3-SiO2 composite was selected to react with 30 bar CO₂ and water at 180°C. Figure 4 shows the XRD patterns of the CaSiO₃-CaCO₃-SiO₂ composite, and the products of the composite reacted with CO₂. The intensity of XRD peaks of CaCO₃ and SiO₂ is obviously increased after the CaSiO₃-CaCO₃-SiO₂ composite reacted with CO₂. Meanwhile, the XRD peaks of CaSiO₃ are weakened.

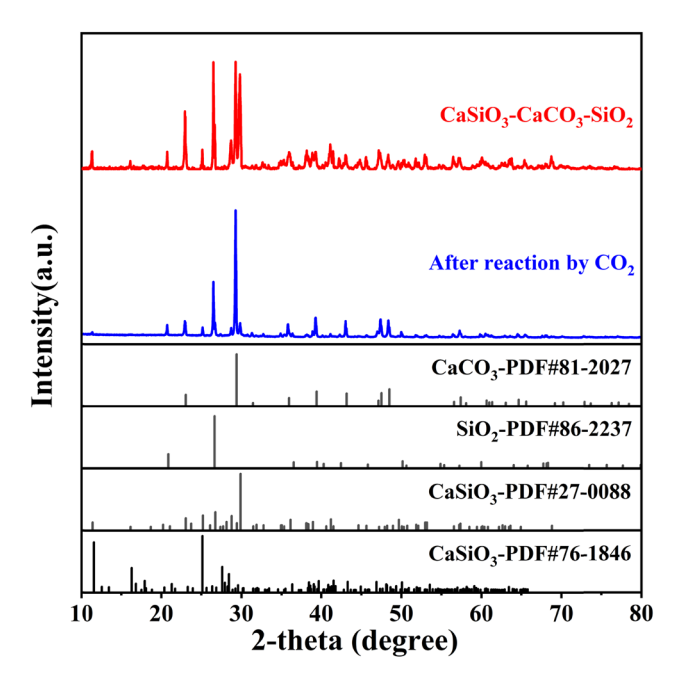


Figure 4: XRD patterns of the $CaSiO_3-CaCO_3-SiO_2$ composite and the products of the composite reacted with CO_2 .

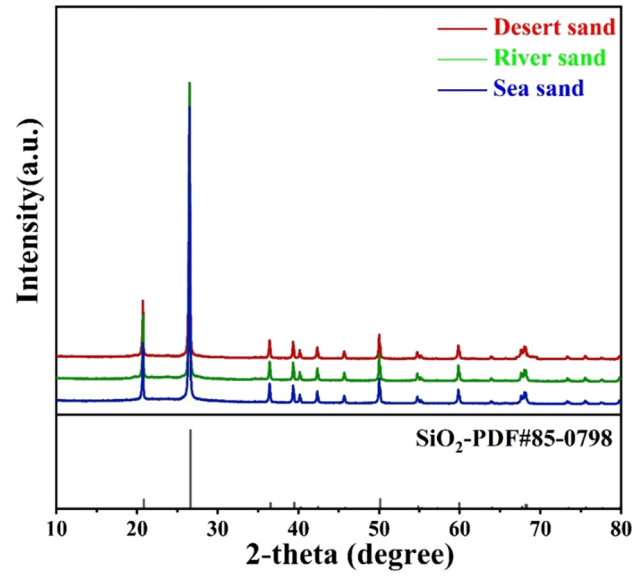


Figure 5: X-ray diffraction analysis of the three kinds of sand in the third experiment.

| Table 4: Energy-dispersive spectrometer analysis of the | e three kinds of sand in Experiment 3 |
|--|---------------------------------------|
|--|---------------------------------------|

| Element | Desert sand | | River sand | | Sea sand | |
|---------|-------------|------|------------|------|----------|------|
| | wt% | at% | wt% | at% | wt% | at% |
| 0 | 52.6 | 65.9 | 53.6 | 67.0 | 50.7 | 64.3 |
| Al | 1.6 | 1.2 | 1.4 | 1.1 | 2.7 | 2.0 |
| Si | 45.8 | 32.9 | 44.6 | 31.8 | 46.1 | 33.4 |
| K | 0.0 | 0.0 | 0.3 | 0.1 | 0.5 | 0.3 |

These results demonstrate the conversion of CaSiO₃ into CaCO₃ and SiO₂ by reacting with CO₂. The chemical reaction can be described by the following equation:

$$CaSiO_3 + CO_2 \rightarrow CaCO_3 + SiO_2$$
 (2)

Based on Eq. 2, it can be seen that the gaseous CO₂ is converted into solid metal carbonates during the reaction with metal silicates. The very low solubility of CaCO₃ and SiO₂ in water is responsible for the increase in the mass of the solid product, resulting in the reduction of silica content of the sand samples that reacted with CO₂. To further remove CaCO₃ from the hydrothermal product, the solid product was soaked and washed with HCl. After purification, the content of SiO₂ in the desert sand is increased to 87.6 wt% (Experiment 2: CO₂@180°C-HCl@25°C), which is higher than that of purification by HCl hydrothermal treatment (Experiment 1), suggesting the efficient conversion from CaSiO₃ and CO₂ to CaCO₃ and SiO₂ (Table 2).

For the river sand, the purity of SiO₂ is 76.6 wt% in Experiment 2 (CO₂@180°C-HCl@25°C), which is lower than that (97.1 wt%) after the HCl treatment in Experiment 1. Similar to the river sand, the SiO₂ content of the sea sand is 79.8 wt% in Experiment 2 ($CO_2@180^{\circ}C$ -HCl@25°C), which is lower than that (90%) after the HCl treatment in Experiment 1. This result can be attributed to the incomplete conversion of CaSiO₃ to CaCO₃ by CO₂ hydrothermal treatment, but it is difficult for HCl to convert residue metal silicates at room temperature. Combined with Table 1, it can be seen that the impurities in the three sands are quite different. For the river sand, the carbon content is the highest among the three sands, representing a high content of carbonate impurities, which can be attributed to the reaction of H₂O and CO₂ in the natural river to promote carbonate deposition in the sand. Unlike freshwater river sand, sea sand is usually soaked and washed by seawater with a high concentration of metal ions, which promotes the deposition of impurity metal ions on its surface and inside, resulting in high metal salt impurities. Therefore, the introduction of high-pressure CO₂ can effectively realize the conversion of metal salts to metal carbonates, especially the conversion of CaSiO₃ to CaCO₃. After the impurities are converted into carbonate, it will be more conducive to the reaction and removal of HCl in the later stage.

To further improve the purity of SiO₂, the Experiment 3 treatment system was used to remove impurities from the sand samples. As shown in Figure 5, only the SiO₂ crystalline phase was identified in the treated product, signifying its high purity. EDS was employed to detect the content of specific elements in the product. As listed in Tables 3 and 4, the atomic number ratios of O to Si are close to 2.0, and the corresponding contents of SiO₂ are 98.4, 98.3, and 96.8%, respectively, for desert sand, river sand, and sea sand. It should be noted that the sand treated by Experiment 3 has higher SiO₂ content compared with those treated by Experiment 1 and Experiment 2 (CO₂@180°C-HCl@25°C), and the content of other metal impurities decreased below 3.2 wt%. Based on the above results, we can confirm that the introduction of CO₂ can effectively convert difficult-to-remove metal salt impurities into easily removable metal carbonates. Benefiting from the transformation of metal salt species, impurities in the sand samples are more easily removed to obtain high-purity SiO₂. The roles of hydrochloric acid and CO₂ are different in the purification of silica from natural sand. High-pressure CO₂ is used to convert difficult-to-remove metal salt impurities into easily removable metal carbonates and silica. Hydrochloric acid is mainly used to react with metal carbonates to convert them into water-soluble chlorides. The metal silicates on the particle surfaces can also react with hydrochloric acid to convert into silica and water-soluble chlorides. Compared with the conventional method, this work provides a green, low-carbon, and energy-saving method.

4 Conclusions

In summary, a facile and universal method to obtain high-purity SiO₂ is developed in this work by introducing high-pressure CO₂ to realize the conversion of difficult-toremove metal salt impurities into easily removable metal

carbonates. Furthermore, HCl hydrothermal and cleaning treatments resulted in a final SiO₂ purity of over 96.8%. This method not only solves the dilemma that the sand purification method is limited by the region, but also improves the purification efficiency of SiO₂, which makes the obtained SiO₂ powder more conducive to the subsequent industrial production and utilization. This study provides a new strategy for the acquisition and utilization of high-purity SiO₂, which will facilitate the transformation of sand in nature to industrialized high-purity SiO₂.

Funding information: This research was funded by National Natural Science Foundation of China (52072342), Natural Science Foundation of Zhejiang Province (LY19E010007), and Scientific Research Foundation of Zhejiang Provincial Education Department (Y202147532).

Author contributions: Jiahui Li: investigation, writing original draft; Yangfeng Wang: investigation, methodology; Xuehua He: investigation, visualization; Qing Sun: formal analysis; Meichai Xiong: investigation; Zichong Chen: data curation, resources; Chengfu Zeng: validation; Xiaohua Zheng: formal analysis; Chu Liang: conceptualization, writing – review and editing, supervision.

Conflict of interest: The authors state no conflict of interest.

Data availability statement: The data generated and analyzed during the study are available from the corresponding author on request.

References

- Zhang C, Liu R, Chen M, Li J, Wang X, Liu Y, et al. Influence of the flocculation effect on the rheological properties of cement slurry. Powder Technol. 2022;398:117118.
- Shiue J, Matthewson MJ, Stupak PR, Rondinella VV. Effects of silica nanoparticle addition to the secondary coating of dualcoated optical fibers. Acta Mater. 2006;54:2631-6.
- Kadari A, Refaei A, Saeed MA. Experimental and theoretical study of the TL process in Nd3+-doped SiO2 optical fibers. Appl Phys A-Mater Sci Process. 2019;125:639.
- Mader M, Schlatter O, Heck B, Warmbold A, Dorn A, Zappe H, et al. High-throughput injection molding of transparent fused silica glass. Science. 2021;372:182-4.
- Putranto AW, Abida SH, Sholeh AB, Azfa HT. The potential of rice husk ash for silica synthesis as a semiconductor material for monocrystalline solar cell: A review. IOP Conference Series: Earth and Environmental Science; 2021. p. 012029.
- Amick IA. Purification of rice hulls as a source of solar grade silicon for solar cells. J Electrochem Soc. 1982;129:864-6.

- Tian L, Shen J, Sun G, Wang B, Ji R, Zhao L. Foliar application of SiO₂ nanoparticles alters soil metabolite profiles and microbial community composition in the pakchoi (Brassica chinensis L.) rhizosphere grown in contaminated mine soil. Env Sci Technol. 2020;54:13137-46.
- Gunay AA, Kim H, Nagarajan N, Lopez M, Kantharaj R, Alsaati A, et al. Optically transparent thermally insulating silica aerogels for solar thermal insulation. ACS Appl Mater Interfaces. 2018;10:12603-11.
- [9] Wang J, Petit D, Ren S. Transparent thermal insulation silica aerogels. Nanoscale Adv. 2020;2:5504-15.
- Ma X, Song Y, Wang Y, Zhang Y, Xu J, Yao S, et al. Experimental study of boiling heat transfer for a novel type of GNP-Fe₃O₄ hybrid nanofluids blended with different nanoparticles. Powder Technol. 2022;396:92-112.
- [11] Xiang S, Zhang YL, Xin Q, Li C. Asymmetric epoxidation of allyl alcohol on organic-inorganic hybrid chiral catalysts grafted onto the surface of silica and in the mesopores of MCM-41. Angew Chem Int Ed. 2002;41:821-4.
- [12] Mihalcik DJ, Lin W. Mesoporous silica nanosphere-supported chiral ruthenium catalysts: Synthesis, characterization, and asymmetric hydrogenation studies. Chemcatchem. 2009;1:406-13.
- [13] Corma A, Garcia H, Moussaif A, Sabater MJ, Zniber R, Redouane A. Chiral copper (II) bisoxazoline covalently anchored to silica and mesoporous MCM-41 as a heterogeneous catalyst for the enantioselective Friedel-Crafts hydroxyalkylation. Chem Commun. 2002;1058-9.
- [14] Maroneze CM, Dos Santos GP, De Moraes VB, Da Costa LP, Kubota LT. Multifunctional catalytic platform for peroxidase mimicking, enzyme immobilization and biosensing. Biosens Bioelectron. 2016;77:746-51.
- Huang R, Shen Y-W, Guan Y-Y, Jiang Y-X, Wu Y, Rahman K, et al. Mesoporous silica nanoparticles: Facile surface functionalization and versatile biomedical applications in oncology. Acta Biomater. 2020;116:1-15.
- [16] Iturrioz-Rodriguez N, Correa-Duarte MA, Fanarraga ML. Controlled drug delivery systems for cancer based on mesoporous silica nanoparticles. Int J Nanomed. 2019;14:3389-401.
- [17] Wang Y, Zhao QF, Han N, Bai L, Li J, Liu J, et al. Mesoporous silica nanoparticles in drug delivery and biomedical applications. Nanomed Nanotechnol Biol Med. 2015;11:313-27.
- [18] Torney F, Trewyn BG, Lin VSY, Wang K. Mesoporous silica nanoparticles deliver DNA and chemicals into plants. Nat Nanotechnol. 2007;2:295-300.
- [19] Chen J, Wang W, Xu Y, Zhang X. Slow-release formulation of a new biological pesticide, pyoluteorin, with mesoporous silica. J Agric Food Chem. 2011;59:307-11.
- [20] Shafiei N, Nasrollahzadeh M, Iravani S. Green synthesis of silica and silicon nanoparticles and their biomedical and catalytic applications. Comments Inorg Chem. 2021;41:317-72.
- Zhang J, Zhang D, Li K, Tian Y, Wang Y, Sun T. N, O and S codoped hierarchical porous carbon derived from a series of samara for lithium and sodium storage: Insights into surface capacitance and inner diffusion. J Colloid Interface Sci. 2021;598:250-9.
- [22] Liu G, Zhao Y, Li J, Zhang T, Yang M, Guo D, et al. Hierarchical N/O co-doped hard carbon derived from waste saccharomyces cerevisiae for lithium storage. J Electroanal Chem. 2022;911:116226-34.

- [23] Meng Y-F, Liang H-J, Zhao C-D, Li W-H, Gu Z-Y, Yu M-X, et al. Concurrent recycling chemistry for cathode/anode in spent graphite/LiFePO₄ batteries: Designing a unique cation/anionco-workable dual-ion battery. J Energy Chem. 2022;64:166-71.
- [24] Morgan DV, Board K. An introduction to semiconductor microtechnology. New York: Wiley; 1990.
- [25] Greenwood NN, Earnshaw A. Chemistry of the Elements. Oxford: Pergamon Press; 1984.
- [26] Lee S. Encyclopedia of chemical processing. US: Taylor & Francis; 2006.
- [27] Chrystie RSM, Ebertz FL, Dreier T, Schulz C. Absolute SiO concentration imaging in low-pressure nanoparticle-synthesis flames via laser-induced fluorescence. Appl Phys B-Lasers Opt. 2019:125:29.
- [28] Romero-Jaime AK, Acosta-Enriquez MC, Vargas-Hernandez D, Tanori-Cordova JC, Pineda Leon HA, Castillo SJ. Synthesis and characterization of silica-lead sulfide core-shell nanospheres for applications in optoelectronic devices. J Mater Sci-Mater Electron. 2021;32:21425–31.

- [29] Nandiyanto ABD, Kim S-G, Iskandar F, Okuyama K. Synthesis of spherical mesoporous silica nanoparticles with nanometer-size controllable pores and outer diameters. Microporous Mesoporous Mat. 2009;120:447–53.
- [30] Wang RL, Zhu YM, Zhang XM, Ji HW, Li L, Ge HY. An economic method for synthesis of highly ordered porous silica. J Colloid Interface Sci. 2013;407:128–32.
- [31] Chun BS, Pendleton P, Badalyan A, Park SY. Mesoporous silica synthesis in sub- and supercritcal carbon dioxide. Korean J Chem Eng. 2010;27:983–90.
- [32] Nishi Y, Doering R. Handbook of semiconductor manufacturing technology. CRC Press; 2000.
- [33] Sun Z, He Y, Wang X, Sun Y, Zheng Z, Xu C, et al. Selective deposition of diamond onto Si substrates using tetraethylorthosilicate SiO₂ films as masks. Thin Solid Films. 1996;289:1–5.
- [34] Rao KS, El-Hami K, Kodaki T, Matsushige K, Makino K. A novel method for synthesis of silica nanoparticles. J Colloid Interface Sci. 2005;289:125–31.